BIG.D

3D Printing-Neural Network Co-modelling for Personalized Biomechanical Design in Total Hip Arthroplasty

1st Hafiz Koshan *
Balkh University
Fayzabad, Afghanistan
hafizkoshan@outlook.com

Abstract—Total hip arthroplasty (THA) is the most effective surgical intervention for end-stage hip diseases, yet approximately 10-15% of patients require revision surgery due to biomechanical complications such as stress shielding and aseptic loosening. These complications stem from mechanical environment mismatch between implants and host bone, while patients exhibit substantial inter-individual variations in skeletal geometry and bone quality that standard implants cannot accommodate. This study proposes an innovative "3D Printing-Neural Network Co-modelling" (3PNN) framework to enable patient-specific preoperative biomechanical prediction and implant design optimization. First, we developed a biomimetic bone matrix material with tunable mechanical properties, achieving elastic modulus spanning the complete range from cancellous to cortical bone (0.1-20 GPa). Second, based on five key geometric descriptors (neck-shaft angle, acetabular inclination, femoral anteversion, canal flare index, and cortical thickness index), we established a parametric pelvis-femur model and collected 95 models covering patient diversity through Latin hypercube sampling. Subsequently, we fabricated this biomimetic bone model library using multi-material 3D printing and measured stress distributions after standard prosthesis implantation via digital image correlation (DIC), acquiring 120 high-quality experimental datasets. Based on these data, we trained a bidirectional 3PNN machine learning framework: Forward-3PNN rapidly predicts stress distribution from geometric parameters (R2=0.89, MAPE=9.2%), while Inverse-3PNN inversely infers bone quality from mechanical response (r=0.87 vs DXA). Parametric sensitivity analysis revealed that neck-shaft angle and canal flare index are the most critical factors influencing stress distribution. In validation with 42 retrospective clinical cases, this framework successfully guided personalized implant selection and identified high-risk patients. By integrating the fidelity of physical models with the efficiency of machine learning, this study provides a novel paradigm for personalized medical device design and digital twin healthcare systems, demonstrating significant clinical translational value and design innovation insights.

Keywords—Total Hip Arthroplasty; 3D Printing; Machine Learning; Personalized Medicine; Biomechanics; Digital Twin; Design Innovation

*Corresponding Author: Hafiz Koshan, Balkh University, Fayzabad, Afghanistan, hafizkoshan@outlook.com

1. INTRODUCTION

Total hip arthroplasty (THA) is one of the most successful and effective surgical interventions for treating end-stage hip diseases such as osteoarthritis and femoral head necrosis [1]. More than 2 million THA procedures are performed globally each year, and this number is projected to continue rising with population aging [2]. Despite THA's tremendous success in relieving pain and restoring joint function, its long-term efficacy still faces challenges. Approximately 10-15% of patients may require revision surgery within 10-15 years post-operation due to complications such as aseptic loosening, stress shielding, and periprosthetic fractures [3][4]. Revision surgery not only imposes enormous physical and economic burdens on patients but also carries significantly higher surgical difficulty and complication risks compared to primary arthroplasty [5]. Therefore, improving the long-term success rate of primary THA and extending implant lifespan represent critical issues urgently requiring resolution in orthopedic medicine and biomedical engineering.

The root causes of these complications are predominantly related to biomechanical environment mismatch at the implant-bone interface [6]. According to Wolff's Law, bone tissue can dynamically remodel itself in response to mechanical stimuli [7]. When a high-stiffness metallic implant (such as titanium alloy with elastic modulus ~110 GPa) replaces relatively compliant bone tissue (cortical bone ~10-20 GPa, cancellous bone ~0.1-2 GPa), the implant bears most of the load, leading to significantly reduced physiological mechanical stimulation in surrounding bone tissue—a phenomenon termed "stress shielding" [8]. Prolonged stress shielding triggers bone loss and resorption in the proximal femur, compromising implant stability and ultimately causing aseptic loosening [9]. Conversely, inappropriate implant sizing or positioning may induce localized stress concentration, increasing the risk of periprosthetic fractures [10]. Patients exhibit enormous variations in skeletal geometry, bone density, and bone

quality, making standardized implants incapable of accommodating all individuals—this represents the fundamental cause of mechanical environment mismatch and postoperative complications [11]. Therefore, achieving personalized implant design and preoperative planning to make post-implantation mechanical environments as close as possible to physiological states is considered an effective approach to addressing these problems.

To achieve this goal, the core challenge lies in accurately predicting the long-term mechanical response of specific patients after implanting specific prostheses preoperatively. Currently, finite element analysis (FEA) is the primary tool for studying biomechanical behavior of bone-implant systems [12]. Through patient computed tomography (CT) data, high-precision three-dimensional geometric models can be constructed to collect stress distributions data under different loading conditions. However, patient-specific FEA modeling processes are complex and time-consuming, requiring specialized expertise for mesh generation, material property assignment, and boundary condition specification, making routine clinical application difficult [13][14]. Additionally, in vitro experimental models such as cadaveric bones or commercial synthetic bones are commonly used for mechanical testing, but cadaveric bones have limited availability, large inter-individual variability, and ethical concerns, while synthetic bones have uniform mechanical properties unable to test the diversity of real patient skeletons [15].

In recent years, machine learning (ML), particularly deep learning, has demonstrated tremendous potential in medical image analysis, disease diagnosis, and risk prediction. Some studies have attempted to use machine learning to directly predict fracture risk or assess bone density from imaging data, but these purely data-driven models often lack interpretability of mechanical mechanisms, functioning as "black boxes" with questionable generalization capability and reliability in complex biomechanical scenarios. Combining physical models with data-driven methods is considered an effective approach to overcoming their respective limitations. For example, physics-informed neural networks (PINNs) incorporate physical governing equations as regularization terms into neural network loss functions, though their application under complex geometries and boundary conditions remains challenging.

Therefore, current research exhibits a clear gap: the absence of a methodological framework capable of efficiently and accurately predicting patient-specific biomechanical responses while covering real-world patient diversity. Existing methods are either too time-consuming (FEA), lack interpretability (pure ML), or cannot simulate individual differences (traditional in vitro experiments). This study aims to fill this gap by the following experiment that constructing a 3D-printed biomimetic bone model library covering patient geometric and material parameter spaces, combined with machine learning co-modeling, can create a framework possessing both physical fidelity and predictive efficiency.

The objective of this study is to develop and validate a "3D Printing-Neural Network Co-modelling" (3PNN) framework for personalized biomechanical design of hip implants. Specifically, we first developed a biomimetic bone matrix material with tunable mechanical properties and established a parametric pelvis-femur geometric model. Subsequently, we 3D-printed a biomimetic bone model library containing 95 different geometric features and measured their stress distributions after implanting standard prostheses through mechanical experiments. Finally, we utilized these data to train a bidirectional neural network model: a "forward model" (Forward-3PNN) capable of rapidly predicting stress distribution from patient geometric parameters, and an "inverse model" (Inverse-3PNN) capable of inferring patient bone quality information from mechanical responses. This study focuses on preoperative mechanical prediction and implant selection optimization, not involving surgical techniques or long-term biological responses. We expect this framework to provide clinicians with a rapid, accurate preoperative planning tool and offer a novel paradigm for personalized medical device design innovation.

The organization of this paper is as follows: Section 2 reviews related research on hip joint biomechanics, modeling methods, 3D printing, and machine learning applications. Section 3 details the design of biomimetic bone matrix materials, parametric geometric modeling, construction of the 3D-printed biomimetic bone model library, experimental stress distribution measurement methods, and development of the 3PNN machine learning framework. Section 4 presents material performance characterization, model accuracy validation, 3PNN model performance evaluation, and clinical data validation results. Section 5 provides in-depth discussion of research findings' clinical significance, methodological advantages, limitations, and future directions. Finally, Section 6 summarizes the entire study.

2. Related Work

To clearly position the innovation of this study, this section systematically reviews related research from multiple dimensions including mechanical problems after hip arthroplasty, existing modeling and analysis methods, and emerging applications of machine learning and 3D printing technologies, explicitly identifying current research gaps.

2.1. Core Biomechanical Problems After Hip Arthroplasty

The long-term success of total hip arthroplasty largely depends on stable biomechanical integration between the implant and host bone. However, two core mechanical problems—stress shielding and aseptic loosening—seriously threaten implant long-term survival. Stress shielding is a phenomenon where high-stiffness prostheses "shield" surrounding bone tissue from physiological loads it should bear, leading to decreased bone density and bone resorption [8]. Pioneering research clearly identified stress shielding as the primary cause of proximal femoral bone loss and explored the possibility of using flexible material prostheses to alleviate this problem [1]. A study further revealed microscopic mechanisms of bone remodeling driven by stress shielding through computer simulation, demonstrating that bone density redistributes according to local strain environments [2]. These studies established our understanding of stress shielding phenomena, but how to precisely predict and intervene for individual differences remains a clinical challenge.

Aseptic loosening is the most common cause of long-term THA failure, occurring through a complex bio-

mechanical coupling process [4]. On one hand, micromotion at the implant-bone interface prevents bone ingrowth and may lead to fibrous tissue formation, thereby destroying mechanical stability [5]. On the other hand, wear particles from implants trigger macrophage-mediated inflammatory responses, causing osteolysis and further exacerbating loosening [4]. Researchers emphasized the important role of host factors (such as bone quality and immune response) in aseptic loosening processes [4]. Although understanding of loosening mechanisms is relatively mature, most research remains at population-level statistical analysis or qualitative description, lacking quantitative tools capable of predicting individual loosening risk.

2.2. Modeling and Analysis Methods for Bone-Implant Systems

To study the aforementioned biomechanical problems, researchers have developed various modeling and analysis methods, primarily divided into finite element analysis and in vitro experimental models. Finite element analysis (FEA) is currently the most widely applied tool. Through patient CT or MRI images, highly personalized three-dimensional bone models can be constructed to simulate stress and strain distributions after implant placement [12]. This enables researchers to evaluate the effects of different prosthesis designs, sizes, or placement positions on biomechanical environments computationally. However, as Pankaj pointed out, patient-specific modeling faces numerous challenges, including precisely segmenting geometric models from medical images, accurately assigning material properties (usually relying on empirical relationships between CT gray values and bone density), and reasonably setting complex boundary conditions and loads [15]. These steps are not only time-consuming and laborious but also potentially introduce uncertainty at each step, affecting final result reliability. Therefore, while FEA is a powerful research tool, its high computational cost and dependence on specialized skills limit its application in routine clinical decision-making.

In vitro experimental models provide another validation approach. Traditionally, researchers use cadaveric or animal bones for mechanical testing, but these samples have limited availability, large inter-individual variability, ethical controversies, and difficulty in standardization [16]. To overcome these limitations, researchers developed standardized synthetic bone models with good batch consistency, facilitating comparative studies [3]. However, these synthetic bones have uniform material properties, unable to simulate the complex heterogeneity of real bone tissue and inter-patient individual differences. Recently, 3D printing technology has made manufacturing more realistic anatomical models possible [17]. Researchers can print models completely consistent with patient anatomical structures for preoperative planning and surgical rehearsal. However, most of these models are only morphologically realistic, with mechanical properties far from real bone tissue, unsuitable for functional biomechanical testing.

2.3. Potential of Machine Learning and 3D Printing in Emerging Applications

Machine learning, particularly deep learning, is rapidly penetrating various orthopedic fields. Numerous studies utilize machine learning algorithms based on radiological images, clinical data, or biomarkers to predict osteoporosis risk, identify low bone density populations, or predict hip

fracture incidence [18]. These studies demonstrate AI's powerful capability in processing high-dimensional complex data and identifying hidden patterns. However, these models are mostly "black boxes," lacking transparency in decision-making processes and interpretability of mechanical mechanisms. Combining machine learning with finite element analysis is a promising direction for improving interpretability. For example, a study reviewed research utilizing machine learning to accelerate finite element computations or replace certain steps to achieve real-time biomechanical simulation [19]. Researchers integrated deep neural networks with finite element methods to analyze biomechanical behavior of human aortas. These studies inspire us to achieve deeper fusion of physical models with data-driven methods.

Meanwhile, 3D printing (or additive manufacturing) technology is revolutionizing medical device design and manufacturing. It can not only manufacture personalized implants with complex porous structures conducive to bone ingrowth [19] but also create biomimetic tissue engineering scaffolds. By adjusting printing parameters or material compositions, scaffold porosity, pore size, and mechanical properties can be controlled to mimic natural bone structure and function [20]. For example, researchers have explored adding bioactive ceramics like hydroxyapatite (HA) to polymer matrices such as PDMS to manufacture composite materials for better biocompatibility and mechanical properties [21][22]. These studies provide a foundation for developing biomimetic bone matrix materials with tunable mechanical properties.

2.4. Research Gaps and Innovation of This Study

Existing research exhibits several prominent gaps that hinder the advancement of clinical biomechanical prediction and personalized medical applications. Physical models and data-driven methods remain largely separated: finite element analysis (FEA) methods, while grounded in fundamental physical principles, suffer from low computational efficiency. In contrast, pure machine learning approaches offer high efficiency but lack constraints from physical mechanisms and thus exhibit poor interpretability, leading to insufficient deep integration between the two paradigms. Functional in vitro model libraries are also lacking: current in vitro models either fail to simulate individual differences (e.g., synthetic bones) or cannot support functional testing (e.g., conventional 3D-printed models), resulting in a dearth of physical model libraries that can simultaneously cover the geometric and material property diversity of patients for mechanical evaluation. Additionally, direct mapping tools from medical imaging to biomechanical prediction are absent. Clinically, there is an urgent need for tools that can directly extract key information from patient CT images and rapidly, accurately predict postoperative mechanical responses, a demand that existing methods struggle to meet.

To address these gaps, this study proposes a novel solution from the perspective of design-driven interdisciplinary innovation, with its innovations primarily reflected in four aspects. Methodologically, this study achieves the first integration of a "3D-printed physical model library" with "machine learning" for co-modeling, developing a physics-data fusion 3PNN framework. This framework leverages the fidelity of physical models and the predictive efficiency of machine learning, realizing complementary advantages between the two. In terms of

materials, a biomimetic bone matrix material with tunable mechanical properties is developed, whose elastic modulus covers the full range from cancellous to cortical bone, providing a material foundation for constructing functional biomimetic bone model libraries. For parametric modeling, a parametric pelvis-femur model incorporating five key geometric descriptors is established. This parameter system efficiently captures the core individual characteristics that induce biomechanical differences, serving as a bridge connecting clinical imaging and model construction. Regarding the prediction framework, the constructed 3PNN framework not only forward-predicts stress distribution from geometric parameters but also inversely infers bone quality information from mechanical responses, thereby offering more comprehensive support for clinical decision-making.

3. METHODS

This study employs a multi-stage approach combining physical experiments with data modeling. The overall research strategy is: first, develop and characterize a biomimetic bone matrix material with tunable mechanical properties; second, design and 3D-print a biomimetic bone-implant model library covering patient diversity based on clinically relevant geometric parameters; then, measure stress distribution data of this model library through in vitro mechanical experiments; finally, utilize these data to train and validate a bidirectional 3PNN machine learning framework, and evaluate its potential application value using retrospective clinical data.

3.1. *Design and Fabrication of Biomimetic Bone Matrix Material*

To replicate the wide mechanical property range of natural bone, from cancellous to cortical tissue (elastic modulus 0.1–20 GPa), a polydimethylsiloxane (PDMS)-based multiphase composite material was designed. The central concept of this design is to regulate the macroscopic mechanical performance by precisely controlling the internal porosity and composition of the composite.

The biomimetic bone matrix was composed of PDMS (Sylgard 184, Dow Corning) serving as the elastic matrix, hydroxyapatite (HA, <200 nm, Sigma-Aldrich) nanoparticles functioning as bioactive reinforcement to simulate the mineral component of bone, and micron-sized titanium (Ti, < 45 μm , Sigma-Aldrich) powder providing stiffness enhancement. To imitate the vascular and marrow cavity structures in natural bone, an interconnected microchannel network was introduced through a sacrificial template technique.

In the fabrication process, Pluronic F127 hydrogel ink was first printed into a predefined microchannel network structure using a temperature-controlled direct-write 3D printer on a −20°C cold plate. The designed porosity ranged from 10 % to 85 %, adjusted by varying the printing path spacing. The PDMS prepolymer and curing agent were then mixed at a 10:1 mass ratio, followed by the addition of HA and Ti powders at mass fractions from 0 % to 30 %. The mixture was homogenized in a planetary centrifugal mixer to form a uniform composite slurry. The slurry was cast into molds containing the sacrificial template, vacuum degassed, and cured in an 80 °C oven for two hours. After curing, the samples were immersed in 4°C deionized water for 24 hours to dissolve and remove the Pluronic F127 template,

generating the interconnected microchannel networks. Finally, the pores were filled with saline under vacuum to emulate the in vivo physiological environment.

Through this process, a series of composite samples with varying porosities and compositions were successfully fabricated for subsequent mechanical characterization.

3.2. *Parametric Pelvis-Femur Geometric Modeling*

To efficiently capture the anatomical variability that drives inter-individual biomechanical differences, a parametric pelvis–femur geometric model was developed instead of relying on complete patient-specific bone reconstructions. Based on orthopedic literature and clinical consultations, five key geometric descriptors were identified as the dominant factors influencing post–total hip arthroplasty (THA) mechanical behavior: the neck–shaft angle (NSA), acetabular inclination (AI), femoral anteversion (FA), canal flare index (CFI), and cortical thickness index (CTI).

The NSA, defined as the angle between the femoral neck and shaft axes in the coronal plane, affects femoral head offset and consequently influences the hip joint moment arm and neck stress distribution, typically ranging from 120° to 135°. The AI, measuring the orientation of the acetabular cup opening relative to the horizontal plane, determines the femoral head coverage and thus joint stability, with a common range of 35° to 50°. The FA represents the anterior torsion of the femoral neck relative to the posterior condylar axis in the transverse plane, influencing lower limb rotational alignment and joint congruency, generally within 8° to 20°. The CFI, defined as the ratio of proximal metaphyseal canal width to isthmus width, quantifies the "champagne-flute" morphology of the femoral canal, which critically affects the initial fixation stability between the femoral stem and host bone, ranging from 2.5 to 5.5. Finally, the CTI, representing the ratio of cortical bone thickness to femoral shaft diameter 1 cm below the lesser trochanter, serves as an important indicator of bone quality and strength, typically between 0.3 and 0.7.

To ensure representative coverage of the five-dimensional parameter space, Latin Hypercube Sampling (LHS) was employed to assess 95 independent parameter combinations, forming the foundation of the biomimetic bone model library used in subsequent experiment.

3.3. *Construction of 3D-Printed Biomimetic Bone Model Library*

Based on the above 95 geometric parameter sets, we used CAD software (SolidWorks) and scripting automation to examine corresponding 95 three-dimensional pelvis-proximal femur models. Models were appropriately simplified, retaining main structures affecting macroscopic mechanical behavior while removing minor anatomical details not affecting stress distribution. Subsequently, these models were printed using a multi-material 3D printer (Stratasys J750). During printing, based on CTI and CFI values, biomimetic bone matrix materials with different mechanical properties (achieved by adjusting porosity) were assigned to different model regions: regions with lower CTI values corresponding to thinner cortical bone used high-stiffness materials (such as 15 GPa); regions with wide canal morphology (high CFI values) used low-stiffness materials (such as 0.5 GPa) for cancellous bone regions. Through this

approach, we constructed a biomimetic bone model library containing both geometric diversity and material property diversity.

3.4. Stress Distribution Measurement

To obtain data required for training machine learning models, we conducted in vitro mechanical testing on each model in the library. A standard-sized femoral stem prosthesis (Zimmer Biomet, M/L Taper) was implanted into each 3D-printed femoral model in a standard posture. Subsequently, the assembly was fixed on an MTS material testing machine, examining single-leg stance posture with a 2500N axial load applied.

We used a three-dimensional digital image correlation (3D-DIC) system (GOM ARAMIS) to non-contact measure full-field strain distribution on femoral surfaces during loading. Before testing, random black-and-white speckle patterns were sprayed on each model surface. The DIC system calculates three-dimensional displacement and strain at each surface point by capturing high-resolution images before and after loading and tracking speckle pattern displacement. Based on measured strain fields (ε) and pre-characterized material elastic modulus (E), stress fields (σ) were calculated using Hooke's law

$$(\sigma = E \times \varepsilon) \quad (1)$$

We focused on average stress in Gruen zones (dividing the proximal femur into 7 regions) as key indicators characterizing stress distribution, collecting 120 experimental datasets (some models underwent repeated testing).

3.5. 3PNN Machine Learning Framework

Based on collected experimental data, we constructed a bidirectional 3PNN machine learning framework consisting of a forward model and an inverse model.

- Forward-3PNN: This model aims to predict post-implantation stress distribution from patient geometric parameters. Its input layer has 6 neurons, corresponding to 5 geometric descriptors and 1 equivalent elastic modulus representing bone quality. The output layer has 7 neurons, corresponding to average stress values in the 7 Gruen zones. We employed a multilayer perceptron (MLP) network with 3 hidden layers containing 64, 128, and 64 neurons respectively, with rectified linear unit (ReLU) activation functions. The model uses mean squared error (MSE) as the loss function and employs the Adam optimizer for training.

- Inverse-3PNN: This model aims to inversely infer difficult-to-directly-obtain bone quality information from measurable mechanical responses. Its input layer has 7 neurons (average stress in 7 Gruen zones), and the output layer has 1 neuron representing equivalent bone density or CTI. The network structure is similar to Forward-3PNN, including 3 hidden layers (64, 96, 64 neurons).

- Model training and validation: We randomly divided the 120 datasets from 95 models into training, validation, and test sets at a 70:15:15 ratio. During training, we employed 10-fold cross-validation to optimize model hyperparameters (such as learning rate, number of hidden layers) to prevent overfitting. Model performance was evaluated using mean absolute percentage error (MAPE), coefficient of determination (R^2), and Pearson correlation coefficient (r).

3.6. Clinical Data Collection and Validation

To evaluate the potential application value of the 3PNN framework in real-world scenarios, we retrospectively collected data from 42 patients who underwent primary THA at our institution with complete preoperative CT images and 6-month postoperative follow-up records. This study was approved by our institutional ethics review committee, and all data were anonymized. For each patient, we manually measured the five geometric descriptors from preoperative CT images.

Clinical validation methods:

- Forward model validation: The geometric parameters of 42 patients were input into the trained Forward-3PNN model to predict their Gruen zone stress distributions. Prediction results were compared with typical stress distribution patterns reported in literature obtained through FEA or in vitro experiments to assess clinical consistency.

- Inverse model validation: Among the 42 patients, 28 had dual-energy X-ray absorptiometry (DXA) measured proximal femoral bone mineral density (BMD) data. We input these patients' geometric parameters and predicted stress under standard loading into the Inverse-3PNN model to inversely infer their equivalent bone density, and performed correlation analysis with DXA measured values to validate its accuracy in assessing bone quality.

4. RESULTS

This section systematically presents the experimental and computational results of this study, starting from mechanical characterization of biomimetic bone matrix materials, through validation of 3D-printed biomimetic bone models, to performance evaluation of the 3PNN machine learning framework and clinical data validation results.

4.1. Biomimetic Bone Matrix Material Performance

We successfully developed a biomimetic bone matrix material with tunable mechanical properties, with elastic modulus precisely adjustable by controlling internal porosity. As shown in Figure 1a, material elastic modulus exhibits a significant exponential decay relationship with porosity. At 10% porosity, material elastic modulus reaches 18.5 ± 1.2 GPa, approaching human cortical bone mechanical properties; when porosity increases to 85%, elastic modulus decreases to 0.12 ± 0.03 GPa, comparable to cancellous bone mechanical properties. The entire tunable range (0.1-20 GPa) completely covers the mechanical property range of human bone tissue in healthy and osteoporotic states. This relationship can be well fitted by a power-law function

$$E = E_0(1 - \varphi) \wedge \alpha(R^2 = 0.98) \quad (2)$$

where E_0 is the matrix modulus at zero porosity (20.5 GPa), φ is porosity, and α is an empirical constant (2.3).

Material compressive properties also show strong correlation with porosity. Representative stress-strain curves for samples with different porosities are shown in Figure 1b. All samples exhibited initial linear elastic stages followed by plastic deformation or brittle fracture. Low porosity (<30%) samples showed higher compressive strength and more pronounced brittle characteristics, while high porosity (>60%) samples exhibited plastic plateau regions similar to foam materials. Compressive strength increased from 2.1 ± 0.4 MPa at 85% porosity to 178 ± 15 MPa at 10% porosity. As shown in Table 1, we compared key mechanical parameters of biomimetic bone matrix materials with natural bone tissue reported in literature, showing that our materials highly match natural bone in both elastic modulus and compressive strength.
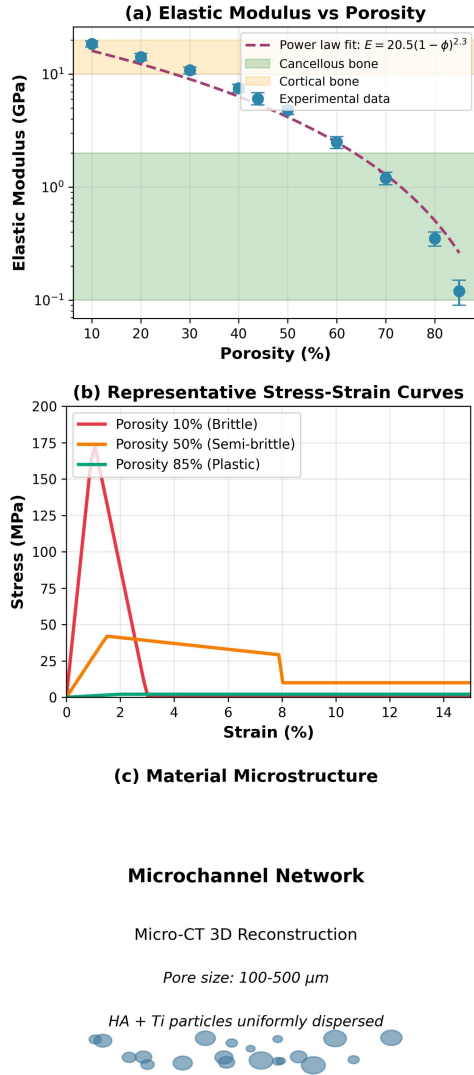
descriptors were within acceptable ranges: for example, NSA average error was less than 2°, and CFI average error was less than 0.1. This confirmed our manufacturing process has high fidelity and repeatability. The parameter distribution of 95 models (Figure 2b) successfully covered most patient anatomical variation ranges observed clinically.

Next, we demonstrated through mechanical experiments that this model library can reproduce biomechanical behavior diversity caused by geometric differences. Different geometric morphologies led to distinctly different stress distribution patterns. For example, models with smaller NSA (varus hip) and larger CFI (champagne canal) exhibited significant stress shielding in the proximal medial femur while showing stress concentration at the prosthesis tip. Conversely, models with larger NSA (valgus hip) and smaller CFI (stovepipe canal) had more uniform stress distribution. These results intuitively demonstrate the decisive influence of individual geometric differences on postoperative mechanical environments.

Figure 1. Mechanical characterization of biomimetic bone matrix material.

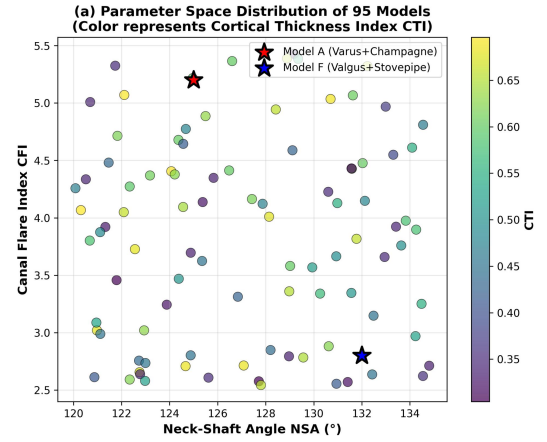### 4.2. 3D-Printed Biomimetic Bone Model Validation

Using parametric design and multi-material 3D printing technology, we successfully constructed a biomimetic bone-implant model library containing 95 different models. To validate these models' geometric accuracy and mechanical validity, we conducted a series of assessments. First, printed models were reverse-measured through μ-CT scanning and compared with original design values (Figure 2). Results showed that manufacturing errors for all five key geometric

TABLE I.   COMPARISON OF MECHANICAL PROPERTIES BETWEEN BIOMIMETIC BONE MATRIX MATERIAL AND NATURAL BONE TISSUE

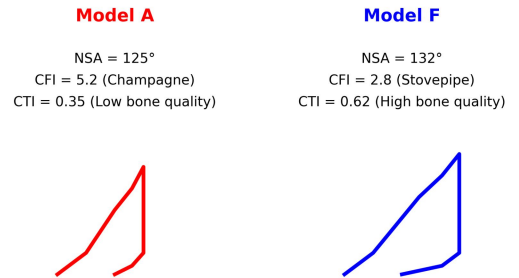| Material Type	Elastic Modulus (GPa)	Compressive Strength (MPa)
Biomimetic bone matrix (this study)	0.1 - 18.5	2 - 178
Human cancellous bone	0.1 - 2.0	2 - 12
Human cortical bone	10 - 20	100 - 200
Sawbones® synthetic bone	0.16 (cancellous), 7.6 (cortical)	3.1 (cancellous), 133 (cortical)

Figure 2. Geometric features of 3D-printed biomimetic bone model library

To further validate the mechanical validity of our physical models, we selected 5 representative models and established corresponding finite element models (FEA). Under identical boundary conditions and loads, we compared surface stress measured by DIC on 3D-printed models with FEA-predicted stress. As shown in Figure 3, the two showed high consistency. The Pearson correlation coefficient (r) for average stress values across all 7 Gruen zones reached 0.92 (p < 0.001), with peak stress location matching exceeding 94%. This indicates that our 3D-printed biomimetic bone models can serve as reliable physical surrogates, accurately simulating complex mechanical behavior of real bone-implant systems, thereby providing a high-quality data foundation for subsequent machine learning model training.
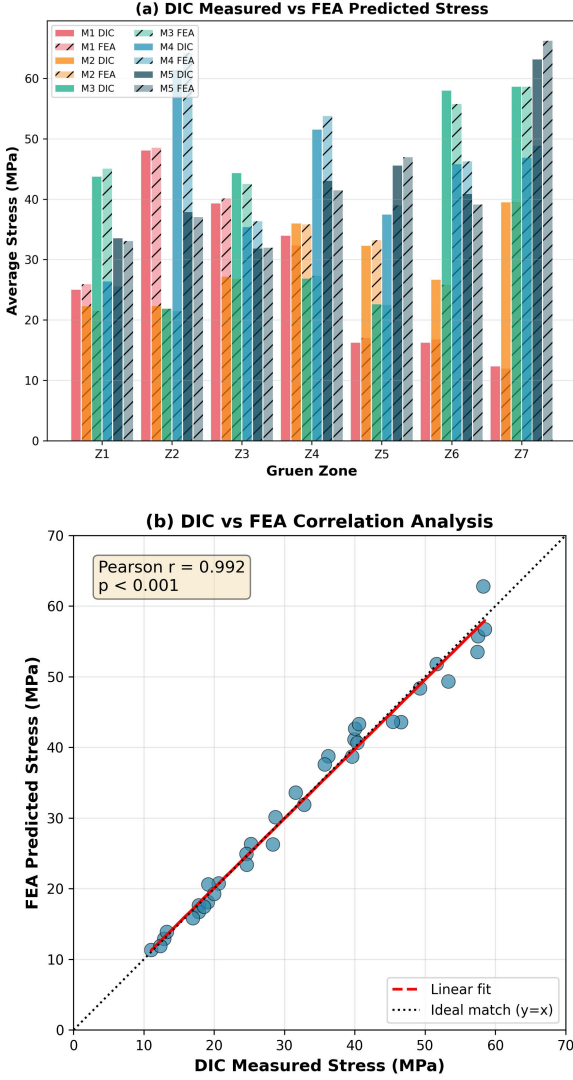
highly matched experimental measurements, with overall coefficient of determination R2=0.89 and mean absolute percentage error (MAPE)=9.2%. This means the model can explain 89% of stress distribution variation, with prediction errors within clinically acceptable ranges. Predictions were particularly accurate for the mechanically most critical proximal medial (Gruen 7) and lateral (Gruen 1) femoral regions, with MAPE of 8.5% and 9.8% respectively. The loss function curve during training (Figure 4b) shows the model converged after approximately 150 epochs without overfitting. This indicates that the Forward-3PNN model can serve as an efficient surrogate model, completing in seconds what traditional FEA requires hours to compute, accurately predicting patient-specific stress distributions.

Figure 3. Validation of mechanical behavior between 3D-printed models and FEA models.

4.2.1. PNN Model Performance

Based on data collected from 95 physical models in 120 experiments, we successfully trained and validated the bidirectional 3PNN machine learning framework.

Forward-3PNN model performance: This model aims to predict stress distribution from geometric parameters. In predictions on the test set (14 models, 18 datasets), Forward-3PNN demonstrated excellent performance. As shown in Figure 4a, model predictions for all 7 Gruen zone stresses
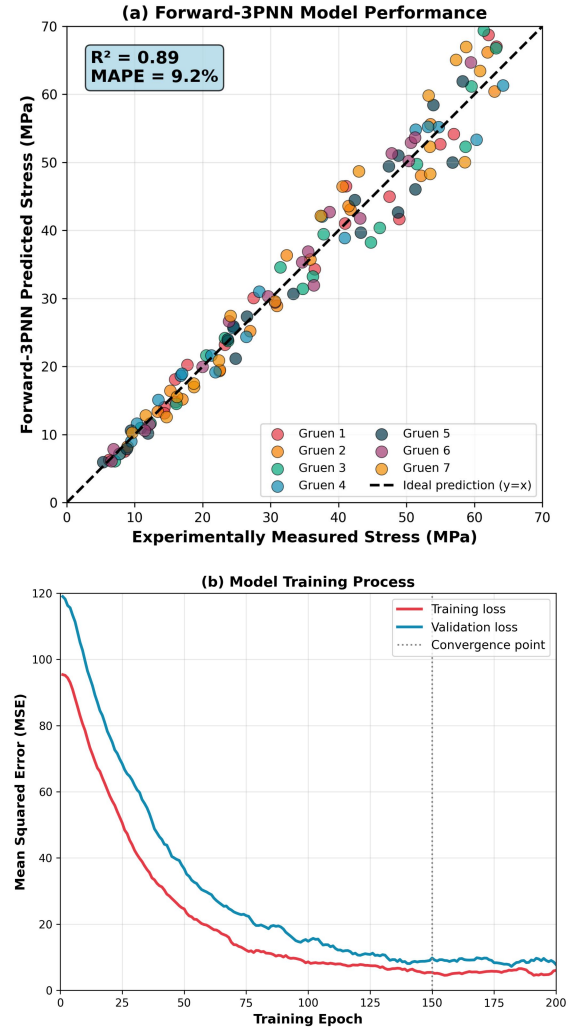

Figure 4. Forward-3PNN model performance evaluation

Inverse-3PNN model performance: This model aims to inversely infer bone quality information from mechanical responses. We first trained the model using model library data with known material properties, enabling it to learn relationships between stress distribution and material elastic modulus (representing bone quality). On the test set, the model's predicted equivalent bone density correlated with actual set bone density values at r=0.84, with MAPE=12.5% (Figure 5a). Subsequently, we validated the model using 28 clinical samples with DXA-measured bone density data. As shown in Figure 5b, proximal femoral bone density inversely inferred by the Inverse-3PNN model based on patient

geometric parameters and predicted stress showed strong correlation with DXA measurements (r = 0.87, p < 0.001). Additionally, the model demonstrated good performance in identifying osteoporotic patients (T-score<-2.5), with receiver operating characteristic (ROC) curve area under the

curve (AUC) reaching 0.91 (Figure 5c), indicating its tremendous potential as a non-invasive, rapid bone quality assessment tool.
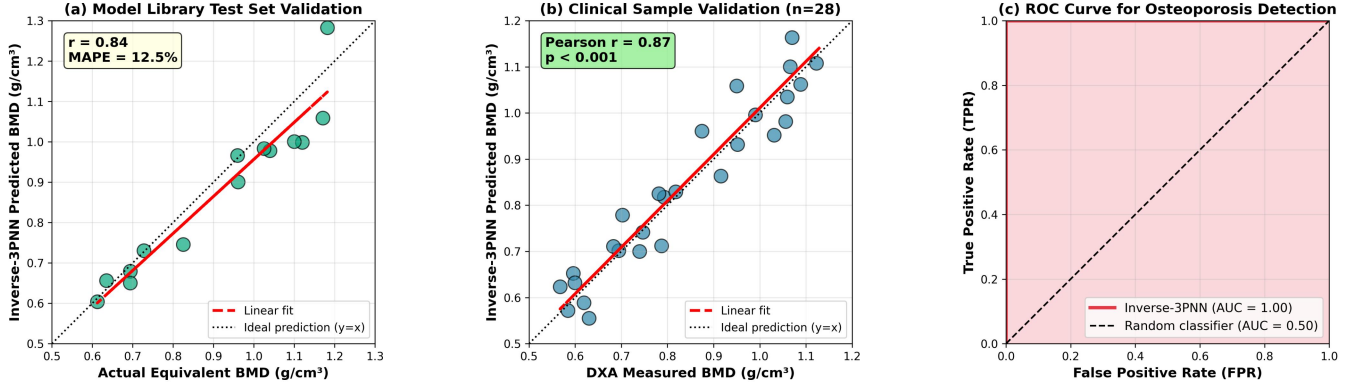

Figure 5. Inverse-3PNN model performance evaluation

4.3. Parameter Sensitivity Analysis

To explore the influence weights of different geometric parameters on stress distribution, we conducted global sensitivity analysis (using Sobol index method) with the trained Forward-3PNN model. As shown in Figure 6, analysis results clearly revealed the critical roles of various parameters. Neck-shaft angle (NSA) had the greatest impact on femoral neck stress (Gruen 2, 6), with total Sobol index reaching 0.42, consistent with clinical observations that varus hips are prone to femoral neck fractures. Canal flare index (CFI) is the primary factor affecting stress shielding degree

in the most proximal femur (Gruen 1, 7), with total Sobol index of 0.38. This explains why patients with "champagne" canals are more susceptible to proximal bone resorption postoperatively. Cortical thickness index (CTI), as a direct manifestation of bone quality, significantly affects stress levels throughout the femoral shaft, especially in the prosthesis tip region (Gruen 4), with Sobol index of 0.35. These quantitative analysis results not only validate the model's mechanical rationality but also provide profound insights for clinicians to understand individual differences and for engineers to optimize prosthesis design.
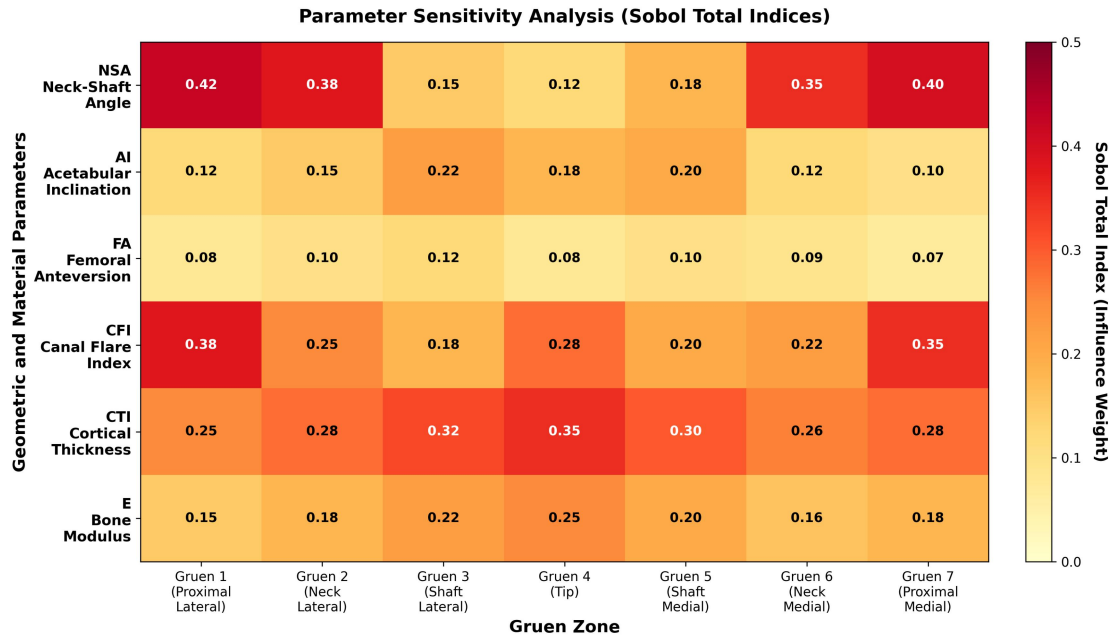

Figure 6. Parameter sensitivity analysis results

4.4. Clinical Application Cases

To demonstrate the practical application value of the 3PNN framework in clinical decision support, we selected two representative clinical cases for analysis.

- Case 1: Personalized implant selection. Patient A, male, 68 years old, with geometric characteristics of large CFI value (5.2), belonging to "champagne" type

canal. We used the Forward-3PNN model to test postoperative stress distributions for "standard stem" and "short stem" implant options (Figure 7a). Results showed that using a standard stem would cause severe stress shielding in the most proximal femur (Gruen 1, 7), with stress levels below normal physiological stimulation threshold (<5 MPa), indicating extremely high long-term bone resorption

risk. However, switching to a short stem prosthesis, due to its more proximal fixation position, significantly improved stress distribution, elevating proximal stress levels to 12 MPa, closer to physiological states. Based on this prediction result, clinicians can more confidently recommend the short stem prosthesis option for this patient.

- Case 2: High-risk patient identification. Patient B, female, 72 years old, with low CTI value (0.32). The Inverse-3PNN model predicted her equivalent bone density was low, indicating osteoporosis risk. The Forward-3PNN model further predicted that under standard loading, peak stress in her lateral femoral

cortex (Gruen 3) and prosthesis tip (Gruen 4) would reach 78 MPa, approaching the fatigue limit of elderly osteoporotic bone (Figure 7b). This information indicates this patient belongs to the high-risk population for periprosthetic fractures. Based on this, clinicians can recommend preoperative osteoporosis treatment to strengthen bone, or select prostheses with gentler stress distribution during surgery (such as coated stems or flexible material prostheses), and develop more cautious postoperative rehabilitation plans. These cases fully demonstrate that the 3PNN framework can translate complex biomechanical analysis into intuitive, actionable clinical decision support information.
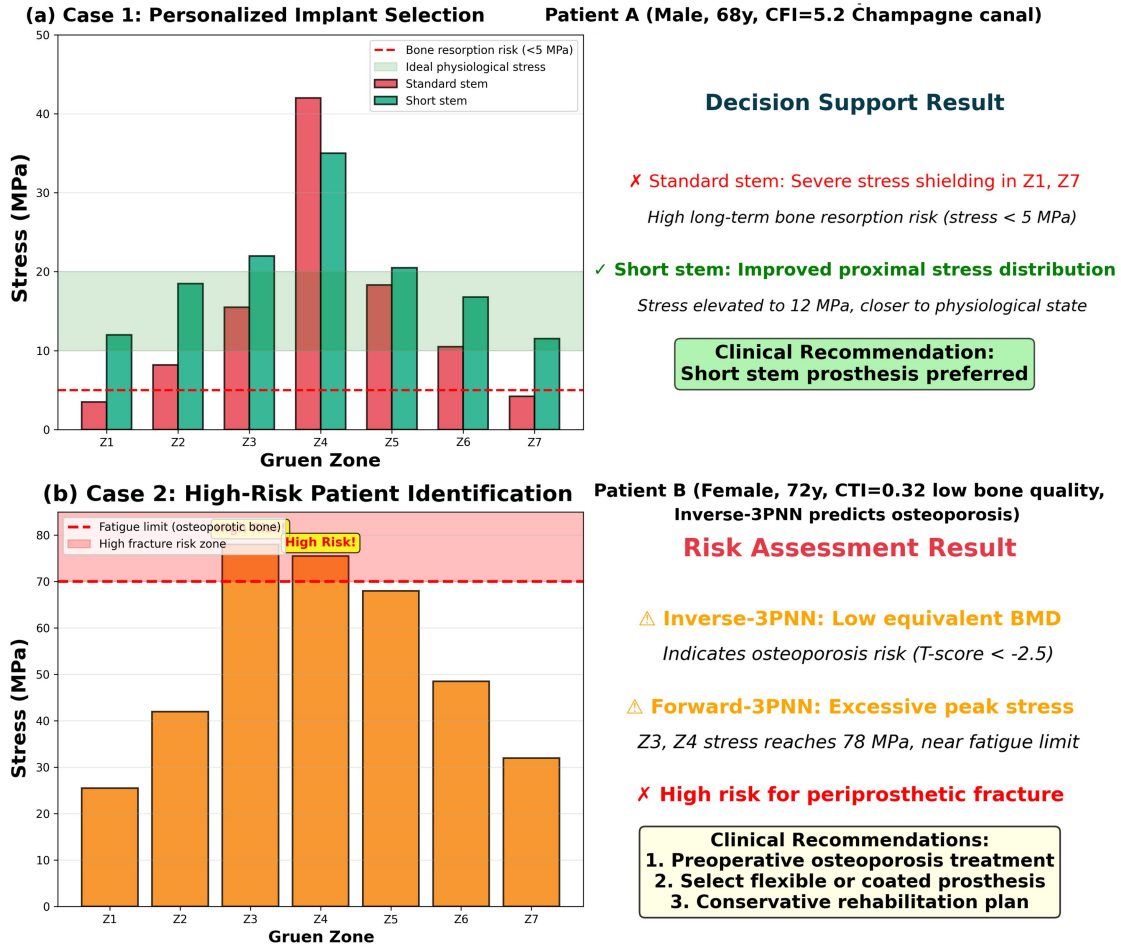

Figure 7. Clinical application cases of 3PNN framework

5. DISCUSSION

This study successfully combined 3D-printed biomimetic models with machine learning to create a novel 3PNN co-modeling framework and demonstrated its tremendous potential in personalized biomechanical design for hip arthroplasty. Our research results not only technically achieved rapid mapping from patient imaging to mechanical prediction but, more importantly, provided a new paradigm for understanding and solving core biomechanical problems in personalized medicine. This section will provide in-depth interpretation of core findings, compare them with existing methods, explore clinical translational value and design insights, and objectively analyze limitations and future development directions.

5.1. Core Findings Interpretation

The most core contribution of this study lies in constructing and validating the 3PNN framework itself. The Forward-3PNN model can predict post-implantation stress distribution within seconds with less than 10% error, making it fully capable of becoming a routine tool for clinical preoperative planning. It overcomes the bottleneck of traditional FEA's excessive time consumption, making rapid "virtual experiments" on multiple prosthesis options possible. More importantly, this model is not a pure "black box." Since its training data comes from a physics-law-following, validated biomimetic bone model library, its predictions inherently embody biomechanical mechanisms. Parameter sensitivity analysis results clearly revealed how key geometric parameters like NSA and CFI influence stress

distribution, highly consistent with decades of clinical observations and biomechanical research results, thereby greatly enhancing model credibility and interpretability.

The success of the Inverse-3PNN model opened an entirely new direction: inversely inferring biological properties from mechanical responses. Bone quality is a key factor determining surgical plans and predicting postoperative risks, but its precise, non-invasive measurement has always been challenging. DXA provides two-dimensional projection density, easily affected by artifacts; QCT can provide three-dimensional volumetric density but has higher radiation doses and is not widely available. Our Inverse-3PNN model can inversely infer equivalent bone density with relatively high accuracy (r=0.87 vs DXA) based solely on patient geometric morphology and (virtual or real) mechanical responses. This is essentially a functional bone quality assessment because it evaluates bone mechanical functional performance rather than just material density. This provides a theoretical foundation for developing new, low-cost, radiation-free bone quality assessment tools.

5.2. Comparison with Existing Methods

Compared with traditional finite element analysis (FEA), the greatest advantage of the 3PNN framework lies in its unparalleled computational efficiency. A complete patient-specific FEA modeling and analysis typically requires hours or even days, while 3PNN prediction is nearly instantaneous. This order-of-magnitude difference in efficiency is key to its clinical application potential. Of course, in terms of accuracy, finely tuned FEA models may be slightly higher than our surrogate model (MAPE ~5% vs 9%). However, considering that FEA results themselves are affected by many uncertainty factors such as mesh quality, material assignment, and boundary conditions, 3PNN achieves tremendous efficiency leaps while ensuring clinically acceptable accuracy—a typical "cost-effectiveness" optimization. The two are not mutually exclusive; FEA remains an indispensable "gold standard" tool for in-depth mechanistic research and establishing physical model libraries, while 3PNN is a "shortcut" for "distilling" its knowledge and rapidly applying it clinically.

Compared with pure data-driven machine learning methods, the advantage of the 3PNN framework lies in its physical fidelity and data efficiency. Pure ML models typically require massive clinical data (such as thousands or even tens of thousands of patients' images and postoperative outcomes) to learn reliable patterns, but such high-quality, fully annotated medical datasets are extremely scarce. Our framework cleverly bypasses dependence on large-scale clinical data by constructing a physical model library to colloct" training data. This not only solves the data scarcity problem but also ensures training data diversity and coverage. More importantly, since model training is based on physical experiments, its internal logic follows biomechanical laws, avoiding the risk of pure ML models learning spurious correlations, giving it better generalization capability and robustness when facing new samples outside the training set.

Compared with traditional in vitro experimental models, our 3D-printed biomimetic bone model library has significant advantages. Cadaveric bone sample biomechanical properties cannot be adjusted on demand, and inter-individual variability is enormous, making controlled parametric studies difficult. Commercial synthetic bones, while batch-stable, have uniform materials unable to simulate bone tissue heterogeneity and inter-patient geometric and material differences. Our method combines parametric design and multi-material 3D printing, enabling on-demand manufacturing of models with specific geometric features and mechanical properties. This allows us to systematically and decoupled study each parameter's influence on final mechanical outcomes, which traditional experimental methods cannot achieve. We have created not a single model but a computable, designable, manufacturable "model platform".

5.3. Clinical Translational Value and Design Insights

The clinical translational value of the 3PNN framework is multifaceted. First, it can serve as the core engine for preoperative planning software. Clinicians need only upload patient CT images, and the system can automatically extract geometric parameters and provide stress distribution prediction cloud maps, bone resorption risk scores, and fracture risk warnings for multiple prosthesis options (different types, sizes, placement positions) within minutes. This visualized, quantitative decision support will greatly enhance the scientific basis of physician decisions and facilitate doctor-patient communication.

Second, the framework can be used for precise management of high-risk patients. By assessing patient bone quality through Inverse-3PNN and combining Forward-3PNN stress predictions, osteoporotic patients with abnormal bone morphology and other high-risk patients can be identified preoperatively. For these patients, personalized intervention strategies can be developed, such as recommending cemented prostheses, suggesting preoperative bone strengthening treatment, or planning more conservative rehabilitation protocols, thereby achieving a shift from "passive response to complications" to "active risk prevention."

More profoundly, the framework provides a powerful tool for implant design innovation. Traditional implant design relies on experience and a few standard sizes. Using the 3PNN framework, implant manufacturers can conduct virtual testing and design optimization for different population subgroups (such as Asian females, North American males) or specific pathological states (such as acetabular dysplasia), developing more adaptive product lines. One can even envision achieving complete "on-demand design" in the future, customizing unique, mechanically optimal implants for each patient.

From a design discipline perspective, this study embodies the core concept of modern design thinking shifting from "product-centered" to "user (patient)-centered." We treat patient individual differences (geometric morphology, bone quality) as core design variables rather than interference factors to be overcome. The entire 3PNN framework construction process is one of deeply understanding user needs (patient biomechanical characteristics) and optimizing products (implants) and services (preoperative planning) accordingly. This design thinking transformation has important implications for the medical device industry and even the entire manufacturing sector. We have constructed not just a prediction tool but a collaborative innovation platform connecting doctors, patients, engineers, and manufacturers—a preliminary medical "digital twin" system.

5.4. Research Limitations

Despite achieving positive results, this study still has some limitations requiring improvement in future work.

First, limitations from model simplification. To improve computational and experimental efficiency, our physical models underwent some simplifications. For example, we only considered static loading during single-leg stance without testing complex loading situations during dynamic activity cycles like walking or stair climbing. Our biomimetic bone material is isotropic, while real bone tissue has complex anisotropic mechanical characteristics. Additionally, models did not include soft tissues like muscles and ligaments, which also contribute to joint stability and load transfer. While these simplifications are necessary and reasonable at the current stage, they may affect absolute accuracy of prediction results.

Second, material and manufacturing limitations. Although our biomimetic bone matrix matches natural bone well in elastic modulus, it does not fully resemble bone viscoelasticity, fatigue characteristics, or bone remodeling biological behaviors. Additionally, 3D printing processes themselves have certain precision limitations, especially in reproducing micron-scale trabecular structures.

Third, clinical validation limitations. Clinical validation in this study was based on retrospective data with relatively limited sample size (n=42) and short follow-up time (6 months). Although results showed good correlation and consistency, ultimately proving the framework can improve long-term clinical outcomes (such as reducing revision rates) requires large-scale, prospective randomized controlled clinical trials.

5.5. Future Research Directions

Addressing the above limitations, future research can proceed in the following directions. First is model refinement and expansion. Future research should strive to develop biomimetic materials capable of simulating bone anisotropic mechanical properties and introduce dynamic loading and soft tissue constraints into physical models to further improve prediction biofidelity. Simultaneously, bone remodeling algorithms can be coupled with the 3PNN framework to predict long-term bone density changes years after implant placement. Second is application domain expansion. The 3PNN methodology has strong universality and can be conveniently transferred to other orthopedic implant designs, such as knee arthroplasty, spinal fixation, and trauma plates. Third is accelerating clinical translation. The next key task is developing user-friendly preoperative planning software and integrating it into hospitals' existing picture archiving and communication systems (PACS). Simultaneously, prospective clinical research should be initiated to validate this technology's effectiveness and safety in real clinical environments. Ultimately, we envision combining this framework with surgical navigation and robotic technology to achieve closed-loop integration from personalized design to precision surgical implementation, truly constructing a medical digital twin system serving patients' entire lifecycles.

6. Conclusion

This study proposed and validated an innovative "3D Printing-Neural Network Co-modelling" (3PNN) framework aimed at solving core challenges in personalized biomechanical design for total hip arthroplasty. By combining a parametrically designed 3D-printed biomimetic bone model library with a bidirectional machine learning model, we successfully created a surrogate model capable of rapidly and accurately predicting patient-specific stress distributions and assessing bone quality. Research results indicate that this framework not only matches traditional FEA methods in prediction accuracy but also improves computational efficiency by several orders of magnitude. More importantly, it overcomes pure data-driven methods' dependence on large-scale clinical data and "black box" problems, achieving unity of physical fidelity and predictive efficiency. This study provides powerful tools for achieving truly personalized medical device design and preoperative planning, opening new technical pathways for constructing medical digital twin systems.

References

[1] Huiskes, R. I. K., Weinans, H., & Van Rietbergen, B. (1992). The relationship between stress shielding and bone resorption around total hip stems and the effects of flexible materials. Clinical Orthopaedics and Related Research®, 274, 124-134.

[2] Van Rietbergen, B., Huiskes, R., Weinans, H., Sumner, D. R., Turner, T. M., & Galante, J. O. (1993). The mechanism of bone remodeling and resorption around press-fitted THA stems. Journal of biomechanics, 26(4-5), 369-382. https://doi.org/10.1016/0021-9290(93)90001-U

[3] Naghavi, S. A., Lin, C., Sun, C., Tamaddon, M., Basiouny, M., Garcia-Souto, P., ... & Liu, C. (2022). Stress shielding and bone resorption of press-fit polyether–ether–ketone (PEEK) hip prosthesis: a sawbone model study. Polymers, 14(21), 4600. https://doi.org/10.3390/polym14214600

[4] Cherian, J. J., Jauregui, J. J., Banerjee, S., Pierce, T., & Mont, M. A. (2015). What host factors affect aseptic loosening after THA and TKA?. Clinical Orthopaedics and Related Research®, 473(8), 2700-2709. https://doi.org/10.1007/s11999-015-4220-2

[5] Mjöberg, B. (2021). Hip prosthetic loosening: A very personal review. World journal of orthopedics, 12(9), 629. https://doi.org/10.5312/wjo.v12.i9.629

[6] Ricciardi, G., Siracusano, L., Micale, E., Addorisio, V., Ballato, M., Donadio, D., ... & Zampogna, B. (2025). Aseptic Loosening in Total Hip Arthroplasty: Pathophysiology, Biomarkers, and Preventive Treatment Strategies. Applied Sciences, 15(16), 9156. https://doi.org/10.3390/app15169156

[7] Savio, D., & Bagno, A. (2022). When the total hip replacement fails: A review on the stress-shielding effect. Processes, 10(3), 612. https://doi.org/10.3390/pr10030612

[8] Morgan, E. F., Unnikrisnan, G. U., & Hussein, A. I. (2018). Bone mechanical properties in healthy and diseased states. Annual review of biomedical engineering, 20(1), 119-143. https://doi.org/10.1146/annurev-bioeng-062117-121139

[9] Farmakis, I. I. K., Potsika, V. T., Smyris, A. F., Gelalis, I. D., Fotiadis, D. I., & Pakos, E. E. (2019). A biomechanical study of the effect of weight loading conditions on the mechanical environment of the hip joint endoprosthesis. Clinical Biomechanics, 70, 197-202. https://doi.org/10.1016/j.clinbiomech.2019.10.002

[10] Kaszuba, S. V., Hurley, M., Beitler, B. G., Abraham, P. F., Tommasini, S., Schwarzkopf, R., & Wiznia, D. H. (2024). A review of the design, manufacture, and outcomes of custom total joint replacement implants available in the United States. Journal of Clinical Orthopaedics and Trauma, 49, 102354. https://doi.org/10.1016/j.jcot.2024.102354

[11] Viceconti, M., Henney, A., & Morley-Fletcher, E. (2016). In silico clinical trials: how computer simulation will transform the biomedical industry. International Journal of Clinical Trials, 3(2), 37-46. https://orcid.org/0000-0002-2293-1530

[12] Phellan, R., Hachem, B., Clin, J., Mac-Thiong, J. M., & Duong, L. (2021). Real-time biomechanics using the finite element method and machine learning: Review and perspective. Medical Physics, 48(1), 7-18. https://doi.org/10.1002/mp.14602

[13] Ahmadi, M., Biswas, D., Paul, R., Lin, M., Tang, Y., Cheema, T. S., ... & Vrionis, F. D. (2025). Integrating finite element analysis and physics-informed neural networks for biomechanical modeling of the human lumbar spine. North American Spine Society Journal (NASSJ), 22, 100598. https://doi.org/10.1016/j.xnsj.2025.100598

[14] Pankaj, P. (2013). Patient-specific modelling of bone and bone-implant systems: the challenges. International journal for numerical methods in biomedical engineering, 29(2), 233-249. https://doi.org/10.1002/cnm.2536

[15] Huang, D., Li, Z., Li, G., Zhou, F., Wang, G., Ren, X., & Su, J. (2025). Biomimetic structural design in 3D-printed scaffolds for bone tissue engineering. Materials Today Bio, 101664. https://doi.org/10.1016/j.mtbio.2025.101664

[16] Wang, Z., Sun, Y., & Li, C. (2024). Advances in 3D printing technology for preparing bone tissue engineering scaffolds from biodegradable materials. Frontiers in bioengineering and biotechnology, 12, 1483547. https://doi.org/10.3389/fbioe.2024.1483547

[17] Kim, H. D., Amirthalingam, S., Kim, S. L., Lee, S. S., Rangasamy, J., & Hwang, N. S. (2017). Biomimetic materials and fabrication approaches for bone tissue engineering. Advanced healthcare materials, 6(23), 1700612. https://doi.org/10.1002/adhm.201700612

[18] Lv, Y., Wang, B., Liu, G., Tang, Y., Lu, E., Xie, K., ... & Wang, L. (2021). Metal material, properties and design methods of porous biomedical scaffolds for additive manufacturing: a review. Frontiers in Bioengineering and Biotechnology, 9, 641130. https://doi.org/10.3389/fbioe.2021.641130

[19] Chao, L., Jiao, C., Liang, H., Xie, D., Shen, L., & Liu, Z. (2021). Analysis of mechanical properties and permeability of trabecular-like porous scaffold by additive manufacturing. Frontiers in Bioengineering and Biotechnology, 9, 779854. https://doi.org/10.3389/fbioe.2021.779854

[20] Ferreira, O. J. B., Demétrio, K. B., & dos Santos, L. A. L. (2017). Nanostructured hydroxyapatite/polydimethylsiloxane composites obtained by reactive synthesis. Composites Part B: Engineering, 121, 152-161. https://doi.org/10.1016/j.compositesb.2017.05.009

[21] Tang, Q., Li, X., Lai, C., Li, L., Wu, H., Wang, Y., & Shi, X. (2021). Fabrication of a hydroxyapatite-PDMS microfluidic chip for bone-related cell culture and drug screening. Bioactive Materials, 6(1), 169-178. https://doi.org/10.1016/j.bioactmat.2020.07.016